ARTICLE
Journal of Cellular Biochemistry 113:2451–2463 (2012)

Journal of Cellular Biochemistry

Reorganization of the DNA–Nuclear Matrix Interactions in a 210 kb Genomic Region Centered on *c-myc* After DNA Replication In Vivo

Rebeca C. Castillo-Mora[1,2] and Armando Aranda-Anzaldo[1,2*]

[1]*Laboratorio de Biología Molecular, Facultad de Medicina, Universidad Autónoma del Estado de México, Paseo Tollocan y Jesús Carranza s/n, Toluca, 50180 Edo. Méx., Mexico*

[2]*Posgrado en Ciencias Biológicas, Facultad de Ciencias UNAM, Universidad 3000 Circuito Exterior S/N, 04510 Ciudad Universitaria, México, D.F., Mexico*

ABSTRACT

In the interphase nucleus of metazoan cells DNA is organized in supercoiled loops anchored to a nuclear matrix (NM). DNA loops are operationally classified in structural and facultative. Varied evidence indicates that DNA replication occurs in replication foci organized upon the NM and that structural DNA loops may correspond to the replicons in vivo. In normal rat liver the hepatocytes are arrested in G0 but synchronously re-enter the cell cycle after partial-hepatectomy leading to liver regeneration. Using this model we have previously determined that the DNA loops corresponding to a gene-rich genomic region move in a sequential fashion towards the NM during replication and then return to their original configuration in newly quiescent cells, once liver regeneration has been achieved. In the present work we determined the organization into structural DNA loops of a gene-poor region centered on *c-myc* and tracked-down its movement at the peak of S phase and after the return to cellular quiescence during and after liver regeneration. The results confirmed that looped DNA moves towards the NM during replication but in this case the configuration of the gene-poor region into DNA loops becomes reorganized and after replication only the loop containing *c-myc* resembles the original in the control G0 hepatocytes. Our results suggest that the local chromatin configuration around potentially active genes constraints the formation of specific structural DNA loops after DNA replication, while in non-coding regions the structural DNA loops are only loosely determined after DNA replication by structural constraints that modulate the DNA–NM interactions. J. Cell. Biochem. 113: 2451–2463, 2012.

KEY WORDS: CHROMATIN; DNA LOOP; HEPATOCYTE; LOOP ATTACHMENT REGION; MATRIX ATTACHMENT REGION; NUCLEAR HIGHER-ORDER STRUCTURE; PARTIAL HEPATECTOMY

In the interphase nucleus of metazoan cells DNA is organized in supercoiled loops anchored to a high-salt insoluble nuclear compartment constituted by a sort of fibrogranular ribonucleoprotein network which retains the shape and some morphological features of the nucleus, known as the nuclear matrix [Razin, 1997; Nickerson, 2001]. The exact composition of the nuclear matrix (NM) is a matter of debate as some 400 proteins have been associated with such a compartment [Mika and Rost, 2005]. Nevertheless there is compelling evidence for the existence of a true nucleoskeleton that involves networks of nuclear filaments and that provides mechanical connectivity and continuity between cytoskeleton and chromatin [Simon and Wilson, 2011]. Moreover, proteins historically regarded as components of the NM participate in the linkage between nucleoskeletal structures and chromatin [Radulescu and Cleveland, 2010]. Currently the NM is understood as a dynamic structural entity [Tsutsui et al., 2005] as exemplified by the fact that important functional nuclear proteins such as topoisomerase II or NeuN/Fox-3 may be shuttling between the NM and the nucleoplasm [Christensen et al., 2002; Dent et al., 2010]. Usually DNA is attached to the NM by non-coding sequences known as matrix associated or matrix attachment regions (MARs). So far in mammals there are no specific consensus sequences for a priori defining an MAR although most well characterized MARs are rich in A-T and repetitive sequences [Ottaviani et al., 2008]. In situ MARs have been operationally classified into constitutive-structural, resistant to high-salt extraction, and facultative, perhaps functional,

Grant sponsor: CONACYT, México; Grant number: 48447-Q-25506.

*Correspondence to: Dr. Armando Aranda-Anzaldo, MD, PhD, Laboratorio de Biología Molecular, Facultad de Medicina, UAEMéx, Paseo Tollocan y Jesús Carranza s/n, Toluca, 50180 Edo. Méx., Mexico. E-mail: aaa@uaemex.mx

Manuscript Received: 16 December 2011; Manuscript Accepted: 27 February 2012

Accepted manuscript online in Wiley Online Library (wileyonlinelibrary.com): 6 March 2012

DOI 10.1002/jcb.24123 • © 2012 Wiley Periodicals, Inc.

non-resistant to high-salt extraction [Razin, 2001; Maya-Mendoza et al., 2003]. Therefore the resulting DNA loops can be also classified into structural and facultative [Elcock and Bridger, 2008; Ottaviani et al., 2008; Rivera-Mulia and Aranda-Anzaldo, 2010]. The high-salt resistant MARs attaching the structural DNA loops to the NM are also known as loop anchorage regions or LARs [Razin, 2001]. The structural DNA–NM interactions occur on a grand scale and so define a nuclear higher-order structure (NHOS). There is evidence that such an NHOS slowly but spontaneously changes in vivo as a function of age [Maya-Mendoza et al., 2005; Alva-Medina et al., 2010, 2011].

For some time it has been speculated that DNA loops correspond to independent functional domains of chromatin. However, it has been shown that a single transcriptional unit may be organized into several structural DNA loops [Iarovaia et al., 2004]. Moreover, the gene *Fyn*, that constitutes a single large transcriptional unit, has been shown to be differentially organized into structural DNA loops according to cell type in vivo without precluding *Fyn* expression [Trevilla-García and Aranda-Anzaldo, 2012]. This evidence rules out a direct correlation between structural DNA loops and transcriptional units. On the other hand, there is varied evidence suggesting that the structural DNA loops may correspond to the actual replicons [Tomilin et al., 1995; Razin, 2001]. Indeed, DNA replication occurs in mammalian cells at so-called replication foci or factories occupying defined nuclear sites at specific times during S phase [Sadoni et al., 2004] and there is important evidence that such replication factories are organized upon the NM [Nakamura et al., 1986; Hozak et al., 1993; Wei et al., 1998]. Theoretical implications resulting from considering the topology of DNA and the actual size of the replication complexes that include enormous polymerizing machines that dwarf the DNA template, suggest that replication of mammalian DNA in vivo involves fixed polymerases in replication foci that reel in their templates as they extrude newly made DNA [Cook, 1999]. This coupled to varied experimental evidence suggests that the NM is the structural support of DNA replication [Anachkova et al., 2005].

Using the model of liver regeneration after partial hepatectomy (PHx) in the rat, we have shown that looped DNA, corresponding to the five structural loops present in 162 kb of the gene-rich region corresponding to the albumin-gene family, moves in a sequential fashion, as if reeled in, towards the NM during DNA replication in vivo. Yet, by day 7 post-partial hepatectomy (7 d post-PHx), once the liver regeneration has been achieved, the DNA returns to its original configuration in the newly quiescent hepatocytes [Rivera-Mulia et al., 2011]. Using the same animal model, in the present work we first determined the organization into structural DNA loops of a 210 kb gene-poor region centered on the *c-myc* gene, region that happened to be organized into at least six well-defined DNA loops in quiescent primary hepatocytes. Then we characterized the dynamics of such structural DNA loops at the peak of DNA replication after PHx. Our experiments confirmed that DNA moves in a sequential fashion towards the nuclear matrix during DNA replication in vivo. However in this case, the movement of DNA to the NM during replication resulted in a permanent reorganization of the structural DNA loops in the *c-myc* genomic region after mitosis and only the loop containing the solitary *c-myc* gene remained closely similar to the original in quiescent, unperturbed, control hepatocytes. Our results suggest that in vivo the local chromatin configuration around active or potentially active genes (such as *c-myc*) tightly constraints the formation of specific structural DNA loops after DNA replication and mitosis, while in non-coding regions the structural DNA loops are only loosely determined after DNA replication by structural constraints that modulate the DNA–NM interactions, thus leading to major reorganization of the local NHOS after mitosis.

MATERIALS AND METHODS

ANIMALS

Male Wistar rats weighing 200–250 *g* were used in accordance with the official Mexican norm for production, care and use of laboratory animals (*NOM*-062-ZOO-1999) and with the approval of the UAEMéx School of Medicine Committee on Bioethics.

PARTIAL HEPATECTOMY

Surgical removal of two-thirds of the liver (partial mechanical hepatectomy) was performed between 9 and 11 am, under ether anesthesia following the classical protocol of Higgins and Anderson [1931]. Briefly, through an abdominal incision the median and left lateral lobes of the rat liver were exposed and a surgical ligature was performed around their base, such lobes were removed (≈70% liver mass) leaving the rest of the liver (right and caudate lobes) intact. Rats were sacrificed using ether anesthesia at 24 h, 7 and 21 days after partial mechanical hepatectomy (PHx). For each experimental series paired rats were subjected to the surgical procedure and one member of the pair was randomly chosen as donor for the liver material post-PHx while the other remained as living proof of the successful regeneration of the liver.

HEPATOCYTES

Primary rat hepatocytes were obtained from rat livers (normal or hepatectomized), as previously described [Maya-Mendoza et al., 2003]. Briefly, the livers were washed in situ by perfusion with PBS without Ca^{2+} and Mg^{2+} (PBS-A) at 37°C for 5 min at 15 ml/min for non-hepatectomized rats and for 2 min for hepatectomized rats. The tissue was further perfused with a solution of collagenase IV, Sigma (0.025% collagenase with 0.075% of $CaCl_2$ in HEPES buffer, pH 7.6) for 8 min for non-hepatectomized rats and for 3 min for hepatectomized rats. Hepatocytes were isolated following the protocol of Freshney [1994]. Viable hepatocytes were counted in a haemocytometer and used immediately for preparing the nucleoids (see below).

PARAMETERS OF LIVER REGENERATION

Liver regeneration progression, including main peak of DNA synthesis and return of hepatocytes to G0 after completion of liver regeneration, was estimated by determination of thymidine kinase activity in the cytosolic liver fraction using a radiometric method as previously described [Morales-González et al., 1999].

PREPARATION OF NUCLEOIDS

The naked DNA loops plus the nuclear substructure constitute a "nucleoid," a very large nucleoprotein aggregate generated by

gentle lysis of a cell at pH 8 in non-ionic detergent and the presence of high salt concentration. Nucleoids were prepared as described previously [Maya-Mendoza and Aranda-Anzaldo, 2003]. Briefly, freshly isolated and washed hepatocytes were suspended in ice-cold PBS-A, aliquots of 50 μl containing 3×10^5 cells were gently mixed with 150 μl of a lysis solution containing 2.6 M NaCl, 1.3 mM EDTA, 2.6 mM Tris, 0.6% Triton-X 100 (pH 8.0). After 20 min at 4°C, the mixture was washed in 14 ml of PBS-A at 4°C for 4 min at 3,000 rpm (1,500 *g*). The pellet was recovered in a volume ranging from 200 to 300 μl.

DNase I DIGESTION OF NUCLEOID SAMPLES

The washed nucleoids were pooled for setting up the DNase I digestion curves (1.8×10^6 nucleoids in 1.2 ml of PBS-A) and mixed with 5 ml of DNase I digestion buffer (10 mM $MgCl_2$, 0.1 mM dithiothreitol, 50 mM Tris at pH 7.2). Digestions were carried out at 37°C with 0.5 U/ml DNase I (Sigma). Each digestion time point aliquot contained 3×10^5 nucleoids. Digestion reactions were stopped by adding 200 μl of stop buffer (final EDTA concentration of 30 mM). The stop buffer contains 0.2 M EDTA and 10 mM Tris at pH 7.5. After digestion with DNase I, the nucleoids' aliquots were pelleted at 9,000 *g* 10 min at 4°C then washed by centrifugation at 9,000 *g* 10 min at 4°C once in PBS-A and twice in double distilled-H_2O water. The NM-bound DNA was determined by spectrometry on aliquots of partially digested nucleoid samples. The final nucleoid pellet was re-suspended in 200 μl double distilled-H_2O to be used directly as template for PCR.

GENOMIC DNA PRIMERS

Distinct pairs of primers were designed for establishing the topological positions relative to the NM of 22 small amplicons located along 210 kb of the genomic region in the rat chromosome 7 centered on the *c-myc* gene (Fig. 1). Briefly, primer pairs were designed approximately each 10 kb in order to establish rather regular intervals along the region studied. All primers sets were designed with a length of 20–25 bp, G–C content between 50% and 55%, T_m of 55–60°C, and PCR products of 275–394 bp (Table I). Secondary structures and dimers/duplexes were avoided.

PCR AMPLIFICATION

Ten nanograms of nuclear matrix-bound DNA were used as template for PCR. PCR was carried out using 0.625 U GoTaq DNA Polymerase (Promega), 1.0 mM $MgCl_2$, 0.1 mM of each dNTP and 10 pmol of each primer in a final volume of 50 μl. Amplification was performed in an Applied Biosystems 2720 thermocycler and the same amplification program was used for all pairs of primers: initial denaturizing step at 94°C for 5 min, denaturizing step at 94°C for 45 s, annealing at 56°C for 30 s, and extension at 72°C for 1 min for 35 cycles, with a final extension at 72°C for 10 min. The identity of all the amplicons was confirmed by restriction analysis with the appropriate restriction enzymes. Amplicons were electrophoresed on 2% agarose gels and visualized using ethidium bromide staining (0.5 μg/ml), recorded and analyzed using a Kodak 1D Image Analysis Software 3.5 system. Amplicons were scored as positive or negative on partially digested nucleoid samples, depending on whether they are detectable by the software using the default settings.

REAL-TIME PCR ANALYSIS OF mRNA

The expression of *PCNA*, *c-myc* and *beta-actin* mRNA was assessed by Real-Time PCR analysis of mRNA using the LightCycler FastStart DNA Master-PLUS SYBR Green 1 kit (Roche) according to the manufacturers instructions in a LightCycler 3.5 thermocycler (Roche). Each reaction used 2 μl of a 1:10 dilution of cDNA. The amplification program was: initial pre-incubation step 95°C 10 min, followed by 45 cycles of touch-down amplification (denaturizing step at 95°C for 10 s; annealing for 10 s and extension at 72°C for 25 s). In the first two cycles annealing was at 65°C and then descending 1°C every two cycles until reaching 60°C. A melting curve was applied at the end of the program for confirming the identity of the amplified product and determining the relative concentration of the template. Primers: *c-myc* forward: TCTGCTCTCCGTCCTATGTTGC; *c-myc* reverse: TTCTTCA-GAGTCGCTGCTGGTG, amplicon size 557 bp. *PCNA* forward: GTGAACCTACAGAGCATGGATTCG; *PCNA* reverse CCACAG-CATCTCCAATATGGCT, amplicon size 373 bp. *Beta-actin* forward: AACACCCCAGCCATGTACG; *beta-actin* reverse: ATGTCACGCAC-GATTTCCC, amplicon size 254 bp.

RESULTS

CORRELATION OF THE KINETICS OF NUCLEOID-DNA DIGESTION WITH THE DNA-REPLICATING STATUS OF HEPATOCYTES

The naked DNA loops plus the NM constitute a nucleoid. Under the conditions of lysis employed to generate nucleoids the DNA remains intact but it lacks the nucleosome structure because of the

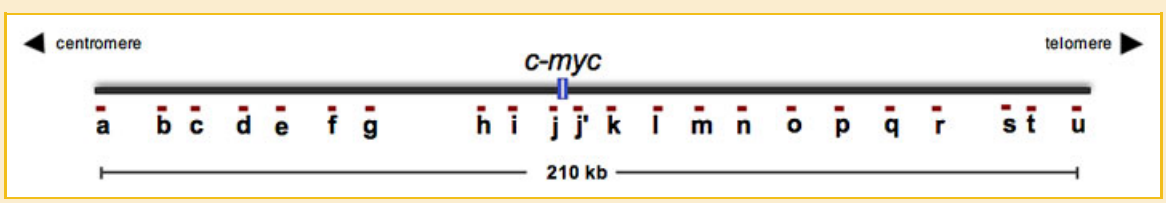

Fig. 1. Target sequences in the 210 kb genomic region centered on *c-myc*. The 210 kb genomic region is located in rat chromosome 7q33. The letters indicate the location of the 22 target DNA sequences (amplicons) to be positionally mapped relative to the NM. The presence of inverted repeats, palindromic and variable sequences, precluded the design of a reliable target amplicon between g and h. The primer pairs defining the corresponding amplicons are given in Table I. [Color figure can be seen in the online version of this article, available at http://wileyonlinelibrary.com/journal/jcb]

TABLE I. Pairs of Primers Used for Amplification of 22 Small Target Sequences (Amplicons) Located Along the 210 kb Genomic Region Centered on *c-myc* (Fig. 1)

Amplicon	Forward primer	Reverse primer	Amplicon length
a	TCACCAGGCTCTCAACACTTTGC	CCTTGATGTCAGGTGTCATAAGGC	394
b	GGAATAACAGGGGAGAGAGAATGG	GCTGGTTGATTGACAGGACTCTGA	393
c	TTCTCACATTCAGGCAACGGTG	CTGCGTGTACCTTTCTTCCTCAAG	342
d	CCACTTCCCATATCTTCCTTCCC	GCAAGTCTGTGATGCTCTGCAA	338
e	CTTACCCTCGTAGCCACATCTTTC	GCTGCTAATGTGAGCCAAACGA	312
f	CTGGCTGCACACATTTGGTCTA	AACCAGTAAGGCTCACAGAGCAAG	290
g	CCTTTACACTGTCTTTACGCTGCC	GTGAAGCCACTGAGACCTCTGTCTA	334
h	GAATGGACAACAGAAACCGAGG	GGACTGAAGGCTCGTGAGATAAAC	291
i	TCCTTGTCTATGGGGAAGCCTGA	CCACCACTACCACTGAGCTAACCTT	341
j	ACTATCACTCCACACTGAGCAAGGG	CCCGACCATTTTCTCCTGCT	282
j′	GGTGCCTCAAGACCTCTAAGTTCC	CTCACTACAACCCTCCGAACCTTT	388
k	ATGCCTTTAATCCCAGAGGTGGAG	GGGTTGAACAGGGTGAGAATGACT	338
l	ATCTTGTGTTCCGCCTGGTACTTG	GAGTCCTCAAATAACAGCCAAGCC	361
m	ACCAAACAAGATCCCACCACTG	GCTCAACTTCATGTTCTCCCTCC	367
n	TAGGCTGTCCCAGGTTTGAAGC	CCAGGATGTTGGTGACACTCAATG	284
o	GCCTCCATAGTACCATGAATGAAAA	GCTCTAATCCCACCTCCTTTGCTA	296
p	GATGCTGAAGATGCTCTCCATCAC	TGAAGATGCTACCTGCCCCTTG	393
q	TCAAGCCCCAGTAAATTCTACCCC	GCAGCAACAAGCAAGAAGTCAGC	304
r	CTAAGTTGGAAAGGGACTTCTGGC	GCACTCAGGAACTCAGGAGACAGA	324
s	TGCTGGGCAAACACTGTACTGA	AGGAATGGGCTAAGAGAGAGGCTA	330
t	CATTTGTAGTCTGTCCCCTGTGAGC	TGCCTGCCTATGACTTCAGAGTCC	275
u	TCACCTCTGTGGGCTAGTGGTAGT	GTTTCCAGCTCACTCATCACCTTC	305

The corresponding amplicon length in bp is indicated.

dissociation of histones and other chromatin proteins. The DNA loops are topologically constrained by being anchored to the NM thus being equivalent to closed DNA circles [Cook et al., 1976; Roti-Roti et al., 1993]. The naked DNA loops display a gradient of supercoiling that goes from lower to higher from tip to base of the loop [Bloomfield et al., 2000], save for the fact that the structural properties of MARs/LARs are such that they also function as buffers or sinks of negative supercoiling [Benham et al., 1997] thus avoiding maximal supercoiling at the base of the loops.

In nucleoid preparations the relative resistance of a given loop-DNA sequence to a limited concentration of DNase I, a non-specific nuclease that is sensitive to the local DNA topology [Lewin, 1980], is directly proportional to its proximity to the NM anchoring point [Maya-Mendoza and Aranda-Anzaldo, 2003; Maya-Mendoza et al., 2004; Rivera-Mulia and Aranda-Anzaldo, 2010]. Two main factors determine such property: (1) steric hindrance resulting from the proteinaceous NM that acts as a physical barrier that relatively protects the naked loop DNA that is closer to the NM from endonuclease action. (2) The local DNA topology, corresponding to the degree of loop DNA supercoiling that is lower in the distal portions of the loop and higher in the regions proximal to the NM. Thus in a large sample of nucleoids exposed to a limited concentration of DNase I there is a consistent trend in which distal regions of the loop are digested first while the regions closer to the NM are digested later.

In the corresponding nucleoid-DNA digestion curves it is possible to calculate the slopes between pairs of digestion-time points (Table II) that together with the standard deviations of the time-point values are used for determining four topological zones relative to the NM (Fig. 2) as previously defined [Rivera-Mulia and Aranda-Anzaldo, 2010; Trevilla-García and Aranda-Anzaldo, 2012]. A topological zone is a relational concept for establishing a range of closeness (in this case for DNA sequences relative to the NM), without considering the actual distance (either in microns or bp), since in topological spaces the notions of distance and length are non-relevant [Flegg, 2001]. There is a fraction of loop DNA that is resistant to DNase I even after long incubation times (the local slope of the digestion curve becomes very close to zero after 60 min and remains unchanged in time), corresponding to the DNA that is actually embedded within the NM and so it is rather inaccessible to the limited concentration of enzyme used (Fig. 2).

In rats the surgical ablation of approximately 70% of the liver mass leads to massive, synchronized re-entry into the cell cycle of some 95% of the residual hepatocytes, this is followed by a well-characterized and highly reproducible large peak of DNA synthesis at 24 h [Michalopoulos and DeFrances, 1997]. The whole regeneration process usually lasts 5–7 days after which there is full recovery of the liver function [Fausto, 2001]. Nucleoids from primary rat hepatocytes isolated at 24 h post-PHx and treated with DNase I show a relatively faster kinetics of loop DNA digestion than the control (compare the corresponding graphs in Fig. 2) indicating greater overall sensitivity of DNA to the endonuclease. This phenomenon has been previously described in nucleoids from cells undergoing

TABLE II. Slopes Between Pairs of Digestion-Time Points in the Corresponding Kinetics of Digestion With DNase I of Nucleoids From Hepatocytes (Fig. 2)

	Slopes			
Digestion time (min)	Control	24 h post-PHx	7 d post-PHx	21 d post-PHx
0–5	−8.9	−10.1	−5.5	−9.8
5–15	−2.0	−2.1	−4.1	−1.5
15–30	−0.4	−0.4	−0.4	−0.2
30–60	−0.1	−0.3	−0.1	−0.2

Control G0 hepatocytes; 24 h post-PHx hepatocytes; 7 d post-PHx hepatocyte; 21 d post-PHx hepatocytes. In all cases the slope after 60 min becomes close to zero and remains unchanged in time.

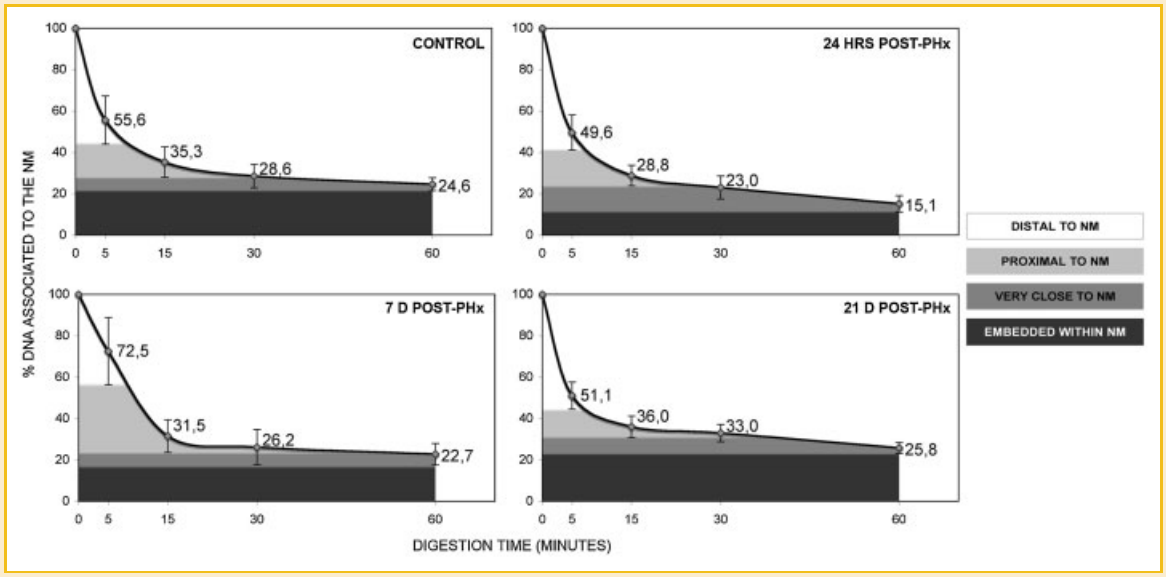

Fig. 2. Kinetics of nucleoid-DNA digestion. Nucleoids from freshly isolated primary rat hepatocytes were digested with a limited concentration of DNAse I (0.5 U/ml) for different times. Each time-point value is the average of separate experiments with samples obtained from separate animals ($n \geq 4$): control G0 hepatocytes. Proliferating hepatocytes 24 h after partial hepatectomy (24 h post-PHx). Restored G0 hepatocytes 7 days after partial hepatectomy (7 d post-PHx). Hepatocytes from fully recovered rats 21 days after partial hepatectomy (21 d post-PHx). Bars indicate the corresponding SD. The topological zones relative to the NM (distal, proximal, very close, and embedded within the NM) correspond to decreasing percentages of total DNA bound to the NM and were defined according to the decreasing slopes between pairs of digestion-time points in each curve (Table II) and the corresponding SD as previously described [Trevilla-García and Aranda-Anzaldo, 2012]. In all cases the slope after 60 min becomes close to zero and remains unchanged in time indicating that the DNA embedded in the NM is rather inaccessible to the limited concentration of the enzyme used.

DNA synthesis [Aranda-Anzaldo, 1992, 1998]. Yet, nucleoids from rat hepatocytes isolated at 7 d and 21 d post-PHx display a kinetics of DNA digestion that is similar to the original in undisturbed G0 hepatocytes and so, the amount of endonuclease-resistant DNA embedded within the NM is basically the same (Fig. 2), indicating that the original degree of supercoiling has been restored in the corresponding structural DNA loops of the newly quiescent hepatocytes in the regenerated liver.

DETERMINATION OF THE ORGANIZATION INTO STRUCTURAL DNA LOOPS OF A GENOMIC REGION CENTERED ON THE *c-myc* LOCUS

We determined, in primary rat hepatocytes, the organization into structural DNA loops of a 210 kb genomic region centered on the *c-myc* gene. For this purpose we used a general method that exploits the topological properties of loop DNA attached to the NM. With this method it is possible to determine the specific DNA loop configuration of a given genomic region of known sequence without previous characterization of the LARs involved [Rivera-Mulia and Aranda-Anzaldo, 2010]. The method is based on the elementary topological principle that points in a deformable string (DNA) can be positionally mapped in space relative to a position-reference invariant (NM), and that from such mapping it can be deduced the configuration of the string in third dimension [Flegg, 2001]. Thus we first designed a set of 21 small amplicons (target sequences) located on average some 10 kb from each other along a gene-poor 210 kb region of rat chromosome 7 centered on the *c-myc* gene (Fig. 1). Within the region studied there is a sub-domain of 23 kb (between the g and h target sequences) in which the DNA sequence is plenty with AT, inverted repeats, palindromic and variable sequences, all these factors precluded the design of a reliable amplicon. Thus it was not possible to have a target sequence within such a sub-domain. Nevertheless, by coupling the specific kinetics of nucleoid-digestion with DNase I (control in Fig. 2) with data from direct PCR amplification of the target sequences in NM-bound templates from partially digested nucleoid samples (control in Fig. 3), corresponding to the time-points of the DNase I digestion curve, it is possible to map the position of each of the target sequences relative to the NM and so to determine its location within a given topological zone (Table III). In the mapping protocol the specific templates are scored either as present (amplifiable) or absent (non-amplifiable) as a function of endonuclease-digestion time, without considering the intensity of the amplicon signals but just whether such signals are detected or not by an image-analysis program since the property of locality in space is factual but not statistical [Maya-Mendoza and Aranda-Anzaldo, 2003; Maya-Mendoza et al., 2004; Rivera-Mulia and Aranda-Anzaldo, 2010; Trevilla-García and Aranda-Anzaldo, 2012]. For most target sequences the consistent amplification pattern among experiments allocated the corresponding sequence to a specific topological zone. However, in about 30–50% of the experiments some target sequences (marked as $+^*$ in Table III) mapped in either of two contiguous topological zones suggesting that the corresponding target sequence is somehow located at the border region or fluctuating between two contiguous topological zones.

The data for the control in Table III were used to draw the most likely DNA loop organization relative to the NM of the region under study in the undisturbed, primary hepatocytes, by considering the distance in kb between the separate target sequences mapped and

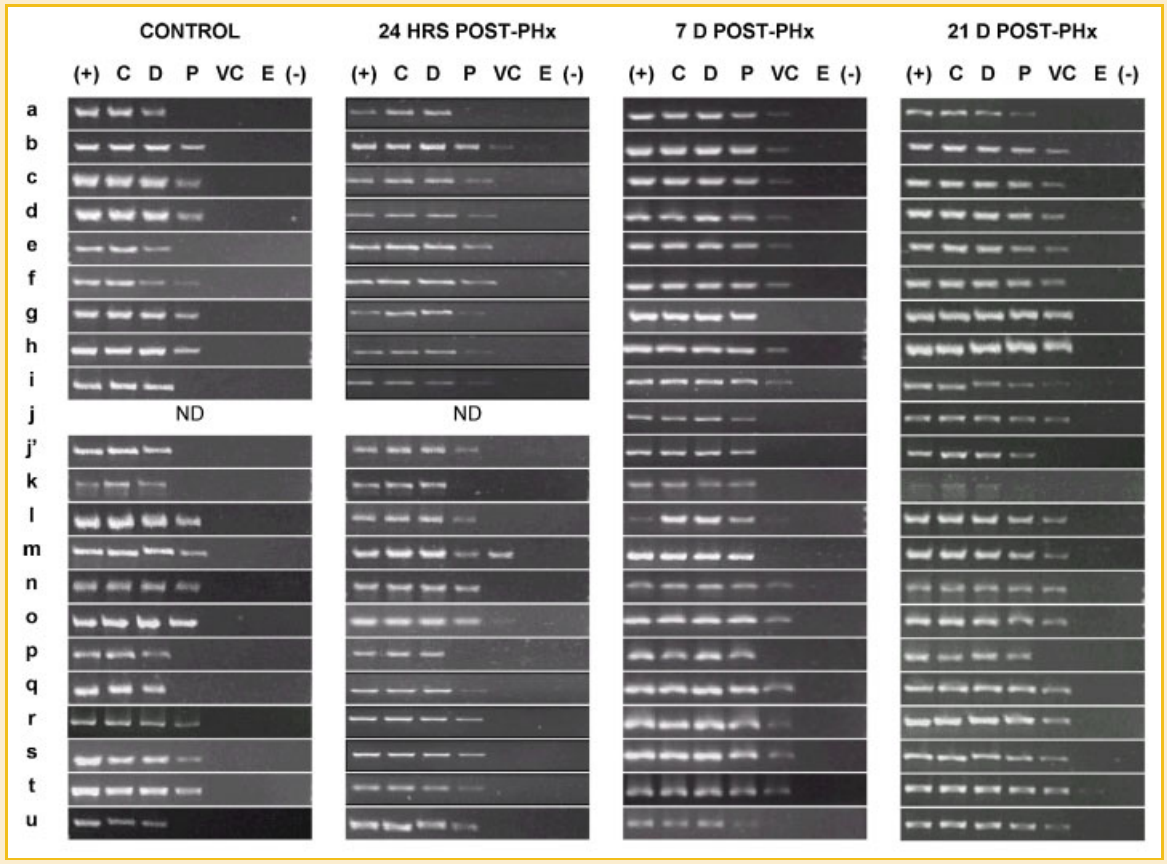

Fig. 3. Positional mapping relative to the NM of specific target sequences. The image shows the results from a typical mapping experiment. The position relative to the NM of specific target sequences along the 210 kb genomic region was determined by PCR. Nucleoids from rat hepatocytes were treated with DNase I (0.5 U/ml) for different times (Fig. 2). The residual NM-bound DNA in the partially digested samples was directly used as template for PCR amplification of the chosen target sequences (a–u). The specific amplicons were resolved in 2% agarose gels and stained with ethidium bromide (0.5 μg/ml). The amplicons were scored either as positive or negative as a function of endonuclease digestion time and for each topological zone relative to the NM, depending on whether or not they were detected by a digital image-analysis system (Kodak 1D Image Analysis Software 3.5) using the default settings (Table III). Topological zones relative to the NM: D, distal; P, proximal; VC, very close; E, embedded within the NM. C, 0′ digestion-time control. (+) positive control (pure genomic DNA as template); (−) negative control (no template). Control G0 hepatocytes; 24 h post-PHx, hepatocytes 24 h after partial hepatectomy; 7 d post-PHx, hepatocytes 7 days after partial hepatectomy; 21 d post-PHx, hepatocytes 21 days after partial hepatectomy. The amplification patterns were consistently reproduced in separate experiments with samples from independent animals ($n \geq 4$). The j amplicon is located near the 5′ of *c-myc* and so it complements amplicon j′ located near the 3′ end of *c-myc*, both amplicons define the location of whole length *c-myc* gene.

the topological positions of such sequences relative to the NM (control in Fig. 4). Thus in primary quiescent hepatocytes the region under study is organized at least in six well-defined structural DNA loops and the *c-myc* gene is contained in a single loop of some 40 kb in whole length (Fig. 4). Given the lack of a reliable target sequence for the region between targets g and h we could not determine whether there are well-defined loops within that 23 kb region or if that region is mostly embedded within the NM. It must be stressed that whichever DNA sequences are actually involved in attaching the DNA to the NM they must lay in the DNA fraction embedded within the NM. However, in our experimental approach there is no need for characterizing the actual LARs involved since the DNA loop organization can be directly inferred from the topological distribution of the target sequences (amplicons) in third-dimensional space. On the other hand, the fact that MARs lack any consensus sequence yet they are usually rich in AT and repetitive sequences precludes, in principle, the design of reliable amplicons that may correspond to or include an actual MAR attached to the NM. Nevertheless when we previously determined the DNA loop organization in the multi-genic locus of the albumin family and the *Fyn* locus in B lymphocytes we found some of the corresponding target amplicons clearly embedded within the NM [Rivera-Mulia and Aranda-Anzaldo, 2010; Trevilla-García and Aranda-Anzaldo, 2012], yet in the present case of the *c-myc* region none of the target amplicons fell within the embedded region in the control hepatocytes.

SEQUENTIAL MOVEMENT OF LOOP DNA RELATIVE TO THE NM CORRELATES WITH DNA REPLICATION

Using nucleoid samples from primary hepatocytes obtained from: control (G0); 24 h post-PHx and 7 d post-PHx livers, we mapped the position relative to the NM of at least 21 target sequences in a comparative fashion. The specific topological zones for each kind of partially digested nucleoid hepatocyte sample were defined according to the specific kinetics of nucleoid DNA digestion shown in Figure 2 (Table III). Figure 3 shows typical amplification patterns

TABLE III. Location of the Target Sequences From the 210 kb Genomic Region Studied Within the Specific Topological Zones Relative to the NM

	Topological zones relative to NM																			
	Control					24 h post-PHx					7 d post-PHx					21 d post-PHx				
Amplicon	C	D	P	VC	E	C	D	P	VC	E	C	D	P	VC	E	C	D	P	VC	E
a	+	+	+*	−	−	+	+	−	−	−	+	+	+	+	−	+	+	+	+*	−
b	+	+	+	−	−	+	+	+	+*	−	+	+	+	+	−	+	+	+	+	−
c	+	+	+	−	−	+	+	+	−	−	+	+	+	+	−	+	+	+	+	−
d	+	+	+	−	−	+	+	+	−	−	+	+	+	+	−	+	+	+	+	−
e	+	+	+*	−	−	+	+	+	−	−	+	+	+	+	−	+	+	+	+	−
f	+	+	+	−	−	+	+	+	−	−	+	+	+	+	−	+	+	+	+	−
g	+	+	+	−	−	+	+	+	−	−	+	+	+	+*	−	+	+	+	+	−
h	+	+	+	−	−	+	+	+	−	−	+	+	+	+	−	+	+	+	+	−
i	+	+	+*	−	−	+	+	+	−	−	+	+	+	+*	−	+	+	+	+	−
j			ND					ND			+	+	+	−	−	+	+	+	+	−
j′	+	+	+*	−	−	+	+	+	−	−	+	+	+	−	−	+	+	+	+*	−
k	+	+	−	−	−	+	+	−	−	−	+	+	+	−	−	+	+	+*	−	−
l	+	+	+	−	−	+	+	+*	−	−	+	+	+	+*	−	+	+	+	+	−
m	+	+	+	−	−	+	+	+	+	−	+	+	+	+*	−	+	+	+	+	−
n	+	+	+	−	−	+	+	+	−	−	+	+	+	+	−	+	+	+	+	−
o	+	+	+	−	−	+	+	+	+	−	+	+	+	+	−	+	+	+	+	−
p	+	+	−	−	−	+	+	−	−	−	+	+	+	−	−	+	+	+	−	−
q	+	+	−	−	−	+	+	+	−	−	+	+	+	+	−	+	+	+	+	−
r	+	+	+*	−	−	+	+	+	−	−	+	+	+	+	−	+	+	+	+	−
s	+	+	+	−	−	+	+	+	−	−	+	+	+	+	−	+	+	+	+	−
t	+	+	+	−	−	+	+	+	−	−	+	+	+	+	−	+	+	+	+	+*
u	+	+	−	−	−	+	+	+	−	−	+	+	+	+*	−	+	+	+	+*	−

Such topological zones were defined according to the specific kinetics of nucleoid-DNA digestion for each kind of nucleoid sample (Fig. 2). The amplicons were scored either as positive or negative as a function of endonuclease digestion time and for each topological zone relative to the NM, depending on whether or not they were detected by a digital image-analysis system (Kodak 1D Image Analysis Software 3.5) using the default settings (Fig. 3). Control G0, samples from normal rat liver hepatocytes. Twenty-four hours post-PHx, samples obtained from hepatocytes 24 h after partial hepatectomy. Seven days post-PHx, samples obtained from hepatocytes 7 days after partial hepatectomy. Twenty-one days post-PHx, samples obtained from hepatocytes 21 days after partial hepatectomy. C, 0′ digestion-time control. D, distal to the NM. P, proximal to the NM. VC, very close to the NM. E, embedded within the NM. All target sequences were mapped in repeated experiments with samples from separate animals ($n \geq 4$). $+^*$ Indicates that in about 30–50% of the experiments the corresponding target sequence mapped to the previous topological zone farther from the NM.

of the corresponding target sequences in DNase I-treated nucleoid samples containing residual loop DNA bound to the NM. With that information we drew the most likely configuration for the corresponding structural DNA loops at 24 h post-PHx and 7 d post-PHx (Fig. 4).

Considering the topological zones defined by the kinetics of nucleoid DNA digestion in samples from undisturbed G0 hepatocytes as the original reference zones and using these zones for calibrating the actual positions relative to the NM of the target sequences in the 24 h post-PHx samples it is possible to confirm a trend for most target sequences to become significantly closer to the NM at 24 h post-PHx (Table IV) when there is a well-known peak of DNA synthesis [Michalopoulos and DeFrances, 1997; Fausto, 2001]. This trend supports our previous observation that DNA moves towards the NM during DNA replication in vivo [Maya-Mendoza et al., 2003; Rivera-Mulia et al., 2011]. However, in the 7 d post-PHx samples, when the liver regeneration is already complete according to classical experimental parameters of liver regeneration (see Materials and Methods Section), most target sequences remain closer to the NM than in the control, indicating that the original configuration of the structural DNA loops has not been restored (Table III). This was in contrast to our published results showing that in the case of the multi-gene locus of the albumin family the original configuration of the structural DNA loops is fully reestablished by 7 d post-PHx [Rivera-Mulia et al., 2011]. Moreover, using the specific kinetics of nucleoid DNA digestion corresponding to G0 (control in Fig. 2) for locating each target sequence within a topological zone relative to the NM in the 7 d post-PHx samples, it was confirmed that most target sequences remained closer to the NM at 7 d post-PHx, without having returned to their original position observed in the unperturbed G0 controls (Table IV).

ORGANIZATION IN STRUCTURAL DNA LOOPS OF THE *c-myc* REGION AFTER FULL RECOVERY FROM PARTIAL HEPATECTOMY

We determined the organization in structural DNA loops of the *c-myc* region in primary hepatocytes obtained at 21 d post-PHx. That means from rats that were fully recovered from the surgical procedure showing normal feeding and overall behavior as well as normal gain of weight. For these experiments we included a further amplicon (j) that is located near the 5′ end of the *c-myc* gene and so it complements the amplicon j′ located near the 3′ end of the *c-myc* gene. This was done in order to assess the location of the whole *c-myc* gene within the topological zones relative to the NM.

Using the corresponding data from: the kinetics of loop DNA digestion with DNase I (Fig. 2), PCR amplification of target sequences in partially digested nucleoid samples corresponding to the time-points of the DNase I digestion curve (Fig. 3), and the location of each mapped sequence within a given topological zone relative to the NM (Table III), we drew the most likely configuration of the DNA loops at 21 d post-PHx (Fig. 4), that together with data in Tables III and IV, confirmed that in the newly quiescent hepatocytes of the regenerated liver most target sequences corresponding to the

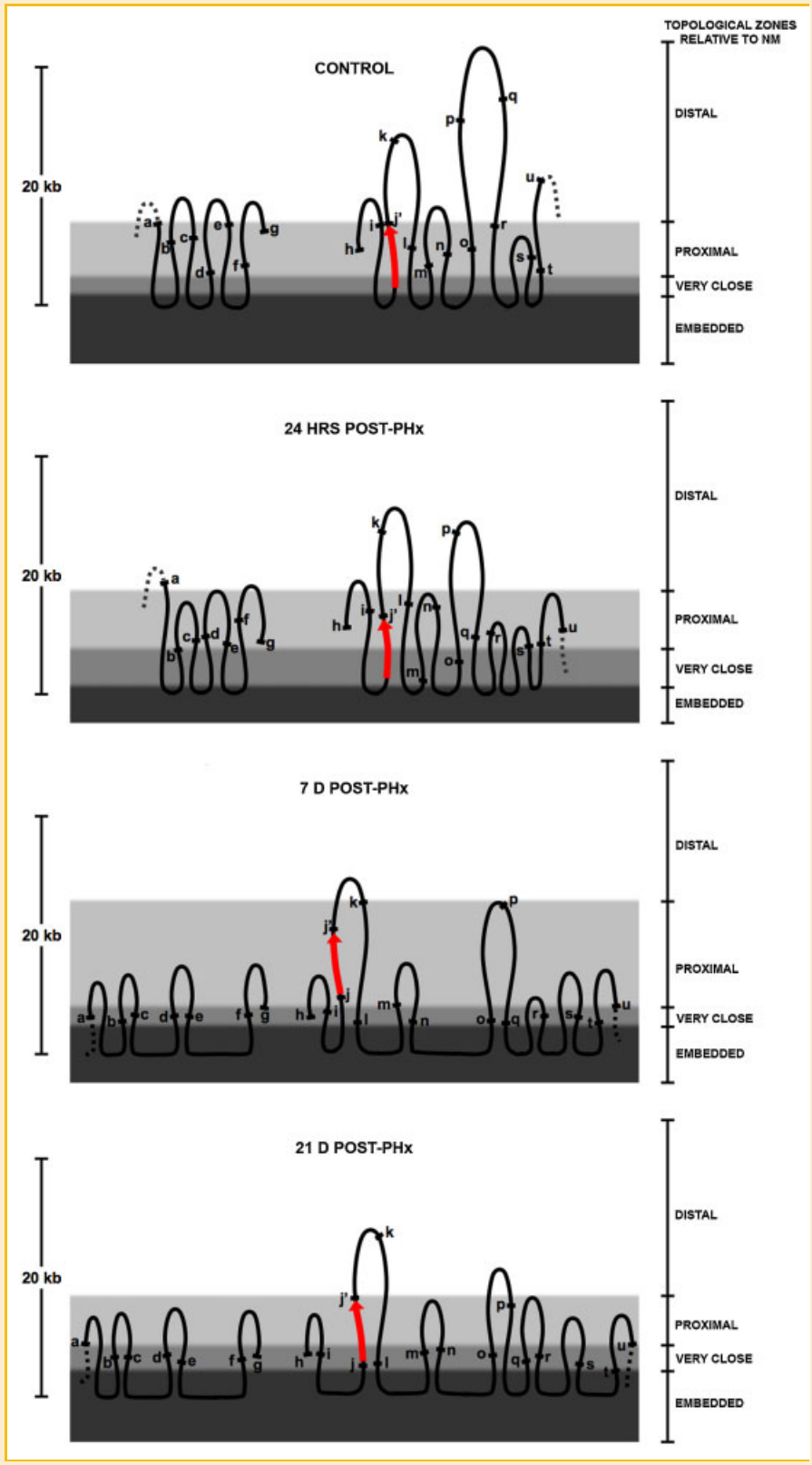

Fig. 4. Experimentally determined structural DNA loop organization of the 210 kb region centered on *c-myc*. The drawings are based on data from Table III. The letters indicate the position of the target sequences within the DNA loops. The arrow corresponds to *c-myc* and the tip indicates direction of transcription. The dashed lines indicate loop regions outside of the region studied. The left bar indicates the relative DNA loop size from tip to base; hence the whole DNA loop length is approximately the double of such value. The right bar indicates the topological zones relative to the NM according to the specific kinetics of nucleoid DNA digestion (Fig. 2). The illustration is according to scale in kb along the x and y axis. [Color figure can be seen in the online version of this article, available at http://wileyonlinelibrary.com/journal/jcb]

TABLE IV. Location of the Target Sequences From the 210 kb Genomic Region Studied Within the Specific Topological Zones Relative to the NM Defined According to the Kinetics of Nucleoid-DNA Digestion in Samples From Control G0 Hepatocytes Obtained From Normal Rat Liver (Fig. 2)

	Topological zones relative to NM according to kinetics of DNA digestion of nucleoids from G0 hepatocytes																			
	Control					24 h post-PHx					7 d post-PHx					21 d post-PHx				
Amplicon	C	D	P	VC	E	C	D	P	VC	E	C	D	P	VC	E	C	D	P	VC	E
a	+	+	+*	−	−	+	+	+*	−	−	+	+	+	+	+*	+	+	+	−	−
b	+	+	+	−	−	+	+	+	+	−	+	+	+	+	+	+	+	+	+*	−
c	+	+	+	−	−	+	+	+	+	−	+	+	+	+	+*	+	+	+	+*	−
d	+	+	+	−	−−	+	+	+	+*	−	+	+	+	+	+*	+	+	+	+*	−
e	+	+	+*	−	−	+	+	+	+	−	+	+	+	+	+*	+	+	+	+	−
f	+	+	+	−	−	+	+	+	−	−	+	+	+	+	+*	+	+	+	+*	−
g	+	+	+	−	−	+	+	+	+	−	+	+	+	+	−	+	+	+	+*	−
h	+	+	+	−	−	+	+	+	−	−	+	+	+	+	+*	+	+	+	+*	−
i	+	+	+*	−	−	+	+	+	−	−	+	+	+	+	+*	+	+	+	+*	−
j			ND					ND			+	+	+	+*	−	+	+	+	+	−
j′	+	+	+*	−	−	+	+	+	−	−	+	+	−	−	−	+	+	+*	−	−
k	+	+	−	−	−	+	+	−	−	−	+	+	−	−	−	+	+	−	−	−
l	+	+	+	−	−	+	+	+	−	−	+	+	+	+	+	+	+	+	+	−
m	+	+	+	−	−	+	+	+	+	+	+	+	+	+	−	+	+	+	+*	−
n	+	+	+	−	−	+	+	+	−	−	+	+	+	+	+	+	+	+	−	−
o	+	+	+	−	−	+	+	+	+	+	+	+	+	+	+	+	+	+	+*	−
p	+	+	−	−	−	+	+	−	−	−	+	+	−	−	−	+	+	+	−	−
q	+	+	−	−	−	+	+	+	+*	−	+	+	+	+	+	+	+	+	+	−
r	+	+	+*	−	−	+	+	+	+*	−	+	+	+	+	+*	+	+	+	+*	−
s	+	+	+	−	−	+	+	+	+*	−	+	+	+	+	+*	+	+	+	+	−
t	+	+	+	−	−	+	+	+	+	−	+	+	+	+	+	+	+	+	+	−
u	+	+	−	−	−	+	+	+	−	−	+	+	+	+	−	+	+	+	−	−

The amplicons were scored either as positive or negative as a function of endonuclease digestion time and for each topological zone relative to the NM, depending on whether or not they were detected by a digital image-analysis system (Kodak 1D Image Analysis Software 3.5) using the default settings (Fig. 3). Control G0, samples from normal rat liver hepatocytes. Twenty-four hours post-PHx, samples obtained from hepatocytes 24 h after partial hepatectomy. Seven days post-PHx, samples obtained from hepatocytes 7 days after partial hepatectomy. Twenty-one days post-PHx, samples obtained from hepatocytes 21 days after partial hepatectomy. C, 0′ digestion-time control. D, distal to the NM. P, proximal to the NM. VC, very close to the NM. E, embedded within the NM. All target sequences were mapped in repeated experiments with samples from separate animals ($n \geq 4$). $+^*$ Indicates that in about 30–50% of the experiments the corresponding target sequence mapped to the previous topological zone farther from the NM.

region under study do not return to their original positions observed in the original, unperturbed G0 hepatocytes. Thus in the case of this 210 kb, gene-poor, genomic region DNA replication resulted in the formation of an extra loop (see 24 h post-PHx in Fig. 4) that was still present in the newly quiescent hepatocytes of the regenerated liver at 7 d post-PHx. Moreover, at 21 d post-PHx the *c-myc* region remains organized into at least seven well-defined DNA loops in the hepatocytes from the regenerated liver and only the loop containing the *c-myc* gene is somehow preserved in a configuration similar to that in the original G0 control hepatocytes (Fig. 4). Indeed, the data suggest that at 7 d post-PHx the whole *c-myc* gene is located in the P region relative to the NM while at 21 d post-PHx the *c-myc* gene is again split between two contiguous topological zones (P and VC) as in the control hepatocytes (Fig. 4).

EXPRESSION OF *PCNA* AND *c-myc* IN HEPATOCYTES BEFORE AND AFTER PARTIAL HEPATECTOMY

PCNA codes for a processivity factor for DNA polymerase delta essential for replication and the abundance of its mRNA increases in cells stimulated to proliferate [Maga and Hubscher, 2003]. On the other hand, *c-myc* is a typical immediate early gene whose expression is augmented by proliferating stimuli [Taub, 1996]. We performed real-time PCR analysis of mRNA experiments for assessing the relative expression of such genes in control (quiescent), 24 h, 7 d and 21 d post-PHx hepatocytes. *PCNA* and *c-myc* are early-response genes necessary for cell proliferation after PHx and so their peak of expression occurs before the entry into S phase which is basically completed by 24 post-PHx [Taub, 1996; Michalopoulos and DeFrances, 1997]. Thus at 24 post-PHx the expression of both genes is already declining. Nevertheless the results show an increase in the corresponding mRNAs at 24 h post-PHx when compared with the control. Such mRNAs have returned to control values by 7 d post-PHx, when liver regeneration is complete (Fig. 5). However, the expression of *c-myc* becomes undetectable at 21 d post-PHx suggesting that the significant reorganization of the loops in the region under study somehow precludes the basal expression of the gene.

DISCUSSION

Metazoan chromosomes correspond to single and very long DNA molecules. The intrinsic structural properties of DNA pose a structural stress problem when the molecule is longer than its currently estimated persistence length of ≈240 pb or 800 A. The persistence length corresponds to that in which the molecule behaves as a rigid rod but at longer lengths the molecule becomes flexible and shows a trend for cyclization [Calladine et al., 2004]. DNA loops are topological equivalents of covalently closed DNA circles. Indeed, by looping and supercoiling around its axis DNA

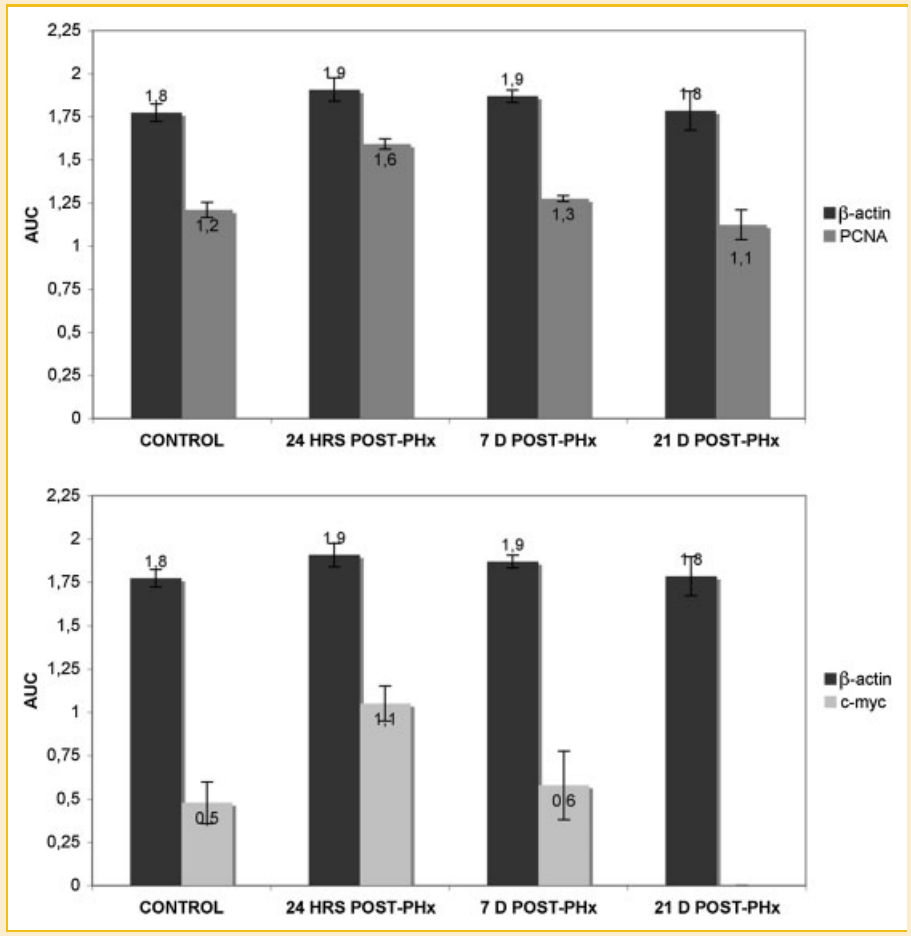

Fig. 5. Real-time PCR analysis of mRNA. Expression of *PCNA* and *c-myc* was analyzed by real-time PCR. Control G0 hepatocytes; proliferating hepatocytes 24 h post-partial hepatectomy (24 h post-PHx); restored G0 hepatocytes 7 days after partial hepatectomy (7 d post-PHx); hepatocytes from fully recovered animals 21 days after partial hepatectomy (21 d post-PHx). The expression of *beta-actin*, a constitutive gene, was included for comparison; *c-myc* expression was not detectable at 21 d post-PHx. AUC: area under the curve. Bars indicate SD ($n = 3$).

dissipates structural-stress energy and avoids the otherwise unavoidable disruption of the weak hydrogen bonds between both strands, thus preserving molecular integrity [Bloomfield et al., 2000; Calladine et al., 2004]. Apparently, the spontaneous formation of loops attached to the NM is a natural answer to a structural stress problem that may put at risk the integrity of DNA. Yet as it has been pointed out elsewhere [Woodcock and Ghosh, 2010] there is common misunderstanding on the phenomenon of DNA looping as some loops are just the result of transient protein-DNA interactions in particular associated with transcription (e.g., enhancer–promoter loops) that involve chromatin proteins and transcription factors while other loops are long-term structures formed independently of chromatin proteins. The present work has been done using nucleoids that consist of the NM plus the naked DNA loops attached to it, such preparations are completely devoid of histones and all other chromatin proteins. Thus here we describe a phenomenology related to naked supercoiled DNA loops attached to a non-soluble proteinaceous structure (NM).

The kinetics of nucleoid DNA digestion with DNase I indicate that similar amounts of total loop DNA are highly resistant to the enzyme and thus embedded within the NM in control, 7 d and 21 d post-PHx samples (Fig. 2). However, at 24 h post-PHx the percentage of loop DNA highly resistant to the enzyme is less than that in the control but in this case there are two factors linked to DNA replication that transiently increase the overall sensitivity of loop DNA to DNase I, an enzyme that hydrolyzes the DNA backbone by a single-strand cleavage (nicking) mechanism [Lewin, 1980]: helicase-mediated reduction of DNA supercoiling and the presence of single-stranded DNA in the replication forks. Nevertheless, at 24 h post-PHx the location of the specific target sequences to a given topological zone was determined using both the zonification according to the specific digestion kinetics (Table III) and the zonification according to the digestion kinetics of the control (Table IV). In both cases the results are consistent with a movement of the target sequences towards the NM in a sequential fashion during DNA replication in vivo (Fig. 4). These results confirm our previous observations concerning the structural DNA loops corresponding to the genomic region of the albumin family [Rivera-Mulia et al., 2011].

It is important to note that we are actually monitoring the average DNA loop configuration in a large number of nucleoids from

hepatocytes. Thus the data for the 24 h post-PHx samples correspond to an average snapshot at the end of the S phase (when most proliferating hepatocytes have incorporated the largest possible amount of $[H]^3$-thymidine), and so to the average configuration at the peak of DNA synthesis [Fabrikant, 1968] of the structural loops in the region studied. Such an average snapshot of the late S phase is possible because of the well-known high synchronicity of reentry into the cell cycle of the remaining hepatocytes after PHx [Fabrikant, 1968; Fausto, 2001]. Under our standard experimental conditions the positional mappings of the target sequences relative to the NM at 24 h post-PHx are quite reproducible among experiments (Fig. 3). However, in experiments carried out at earlier and latter hours around the main peak of DNA synthesis (24 h post-PHx) the location of most target sequences relative to the NM becomes truly erratic (data not shown), yet this indirectly confirms the movement of DNA towards the NM during S phase.

The loop organizations depicted in Figure 4 were inferred from the distribution in topological space of a relatively large set of points (amplicons) rather evenly spaced along the genomic region studied. So far there is non-reliable method for actually seeing the specific loops corresponding to a natural genomic region. Currently 3C chromosome conformation capture (3C) is widely used for determining whether any two DNA sequences are located in spatial proximity to each other in the eukaryotic nucleus [Woodcock and Ghosh, 2010]. This method is based in the artificial crosslinking between DNA and proteins within the nucleus followed by digestion of chromatin with restriction enzymes and partial solubilization of chromatin fragments and dispersion by dilution. Then enzymatic ligation of DNA fragments held in proximity is carried out followed by identification of such fragments by different means. So far only a single study of 3C applied to preparations extracted for NM, hence devoid of chromatin proteins (M3C), has been published and the results showed that important DNA sequences labeled as proximal to each other in the standard 3C protocol were not so in the M3C assay [Gavrilov et al., 2010]. Yet despite its uncertainties many a scientist infer that a DNA loop exists between two DNA sequences positive in the artificial proximity ligation procedure of 3C. Hence the whole trajectory of a several-kb long segment of DNA in space is inferred from just the proximity of two points (short DNA sequences). In contrast, our topological approach for determining the organization into structural DNA loops of any genomic region with known sequence [Rivera-Mulia and Aranda-Anzaldo, 2010] is based in a sound, fundamental topological principle [Flegg, 2001]: points in a deformable string (DNA) can be positionally mapped in topological space relative to a position-reference invariant (NM), from such mapping it can be deduced the trajectory of the string in third dimension. Corollary: the larger the number of points mapped (short DNA sequences) the better the resolution of the strings' trajectory. Hence we do not depend on pairs of apparently proximal points (two short DNA sequences) for assuming that there is a loop between each pair but we map in topological space a set of points (short DNA sequences) whose distribution depicts the whole trajectory of the string (genomic region) in space.

In the case of the c-*myc* region the original position of most target sequences relative to the NM (control in Fig. 4) was not recovered in the newly quiescent hepatocytes at 7 d nor at 21 d post-PHx despite the successful regeneration of the liver (Tables III and IV). Indeed, the resulting configuration for most of the structural DNA loops was remarkably different to that in the control (Fig. 4). Interestingly, at 21 d post-PHx only the loop containing the *c-myc* gene is rather similar to the original in the control hepatocytes. In the rat *c-myc* is a solitary gene located in chromosome 7q33, the nearest bona fide genes are *A1bg* located some 1.15 Mb from the 5′ end of *c-myc* and *Gsdmc 1* located some 2.15 Mb from the 3′ end of *c-myc* (RGSC Genome Assembly v3.4). Hence, the fact that a gene-rich genomic region recovers its original configuration of structural DNA loops after liver regeneration [Rivera-Mulia et al., 2011] while this is not the case for a gene-poor region as the one centered on *c-myc*, suggests that the chromatin conformation around potentially active genes somehow determines or guides the reestablishment of the DNA–NM interactions after DNA replication and mitosis. This suggestion is further supported by the fact that the original loop containing *c-myc* is the only one that is relatively preserved in the newly formed hepatocytes after liver regeneration and so it remains rather heterogeneous in size relative to its neighbors (Fig. 4). Nevertheless, the apparent permanent reorganization of the *c-myc* genomic region following DNA synthesis and mitosis during liver regeneration correlates with the eventual extinction of *c-myc* basal expression in the regenerated liver (Fig. 5). As *c-myc* is an early response gene necessary for cellular progression to mitosis, the absence of basal *c-myc* expression in hepatocytes from regenerated liver may be also correlated with the known fact that rats that have previously undergo a full cycle of liver regeneration may undergo further rounds of liver regeneration but each further round is more protracted and less efficient [Michalopoulos and DeFrances, 1997] as if *c-myc* upregulation after PHx starts from zero in the regenerated liver.

DNA–NM interactions of the structural kind occur on a grand scale as there are some 66,000 DNA loops in a typical diploid hepatocyte of a young rat. Yet that number tends to increase in the long term as a function of age, with the corresponding reduction in the loop average size [Maya-Mendoza et al., 2005]. This phenomenon, apparently driven by thermodynamic and structural constraints, has been linked to the loss of proliferating potential and terminal differentiation of mammalian cells after which the loops become quite short and homogeneous in size [Aranda-Anzaldo, 2009; Alva-Medina et al., 2010, 2011]. However, from our previous work we know that a time window of not more than 21 d post-PHx, used in the present experiments, is not long enough for producing spontaneous but observable changes in the overall NHOS of hepatocytes [Maya-Mendoza et al., 2005]. Therefore, the observed reorganization of the structural DNA loops in the *c-myc* region is a consequence of DNA replication and mitosis after PHx. For obvious ethical reasons we cannot perform repeated PHx in the same animal yet it is known, from old reports in the literature, that young adult rats may undergo repeated PHx followed by the corresponding successful liver regeneration [Michalopoulos and DeFrances, 1997] and so this implies that whichever the resulting NHOS after liver regeneration in young rats such an NHOS is compatible with further DNA replication in vivo.

It is known that a single, large transcriptional unit can be differentially arranged into several DNA loops according to cell type without precluding the expression of the corresponding gene, indicating that transcription is not a major factor for determining the structural DNA loops [Trevilla-García and Aranda-Anzaldo, 2012]. Indeed, chromatin proteins do not participate in the DNA–NM interactions as such proteins are completely eliminated by the high salt used for obtaining nucleoids [Verheijen et al., 1986]. Thus, the structural DNA–NM interactions have a higher affinity than those between chromatin proteins and DNA. Nevertheless, in vivo chromatin proteins may hinder potential DNA–NM interactions by competing with the NM for a given DNA sequence or configuration. Hence the chromatin conformation around potentially active genes may contribute to the selection of the actual set of LARs from the potential set of MARs in a gene-rich region, thus leading to a local NHOS that remains rather similar through several cell cycles. On the other hand, in a gene-poor region the average chromatin conformation associated with non-coding DNA seems unable to compete with the NM for DNA sequences or configurations and so after DNA replication or mitosis the reestablishment of DNA–NM interactions in a non-coding genomic region may be primarily guided by structural constraints resulting from torsional and bending stress along the DNA, stress that needs to be dissipated in order to preserve the structural integrity of DNA and this would lead to major reorganization of the local DNA–NM interactions.

ACKNOWLEDGMENTS

While doing this work Rebeca C. Castillo-Mora was a CONACYT Research Scholar within the Graduate Program in Biological Sciences at the Faculty of Sciences-UNAM, México. We thank Dr. Rolando Hernández-Muñoz from IFC-UNAM and Dr. Federico Martínez from the Faculty of Medicine-UNAM for their valuable comments and suggestions on this work.

REFERENCES

Alva-Medina J, Dent MAR, Aranda-Anzaldo A. 2010. Aged and post-mitotic cells share a very stable higher-order structure in the cell nucleus in vivo. Biogerontology 11:703–716.

Alva-Medina J, Maya-Mendoza A, Dent MAR, Aranda-Anzaldo A. 2011. Continued stabilization of the nuclear higher-order structure of post-mitotic neurons in vivo. PLoS ONE 6(6):e21360.

Anachkova B, Djeliova V, Russev G. 2005. Nuclear matrix support of DNA replication J Cell Biochem 96:951–961.

Aranda-Anzaldo A. 1992. Early induction of DNA single-stranded breaks in cells infected by herpes simplex virus type 1. Arch Virol 122:317–330.

Aranda-Anzaldo A. 1998. The normal association between newly replicated DNA and the nuclear matrix is abolished in cells infected by herpes simplex virus type 1. Res Virol 149:195–208.

Aranda-Anzaldo A. 2009. A structural basis for cellular senescence. Aging 1:598–607.

Benham C, Kohwi-Shigematsu T, Bode J. 1997. Stress-induced duplex destabilization in scaffold/matrix attachment regions. J Mol Biol 2774: 181–196.

Bloomfield VA, Crothers DM, Tinoco I, Jr. 2000. Nucleic Acids; structure, properties and functions. Sausalito, CA: University Science Books. pp. 443–473.

Calladine CR, Drew HR, Luisi BF, Travers AA. 2004. Understanding DNA. London: Elsevier-Academic Press. pp. 94–138.

Christensen MO, Larsen MK, Barthelmes HU, Hock R, Andersen CL, Kjeldsen E, Knudsen BR, Westergaard O, Boege F, Mielke C. 2002. Dynamics of human toposiomerase II alpha and II beta in living cells. J Cell Biol 157:31–44.

Cook PR. 1999. The organization of replication and transcription. Science 282:1790–1795.

Cook PR, Brazell I, Jost E. 1976. Characterization of nuclear structures containing superhelical DNA. J Cell Sci 22:303–324.

Dent MAR, Segura-Anaya E, Alva-Medina J, Aranda-Anzaldo A. 2010. NeuN/Fox3 is an intrinsic component of the neuronal nuclear matrix. FEBS Lett 584:2767–2771.

Elcock LS, Bridger JM. 2008. Exploring the effects of a dysfunctional nuclear matrix. Biochem Soc Trans 36:1378–1383.

Fabrikant J. 1968. The kinetics of cellular proliferation in regenerating liver. J Cell Biol 36:551–565.

Fausto N. 2001. Liver regeneration: From laboratory to clinic. Liver Transplant 7:835–844.

Flegg HG. 2001. From geometry to topology. Mineola, NY: Dover Publications. 208 pp.

Freshney I. 1994. Culture of animal cells, 3rd edition. New York: Wiley-Liss. pp. 320–322.

Gavrilov AA, Zukher IS, Philonenko ES, Razin SV, Iarovaia OV. 2010. Mapping of the nuclear matrix-bound chromatin hubs by a new M3C experimental procedure. Nucleic Acids Res 38:8051–8060.

Higgins GM, Anderson RM. 1931. Experimental pathology of the liver. I. Restoration of the liver of the white rat following partial surgical removal. Arch Pathol 12:186–202.

Hozak P, Hassan AB, Jackson DA, Cook PR. 1993. Visualization of replication factories attached to nucleoskeleton. Cell 73:361–373.

Iarovaia OV, Bystritsky A, Ravcheev D, Hancock R, Razin SV. 2004. Visualization of individual DNA loops and a map of loop domains in the human dystrophin gene. Nucleic Acids Res 32:2079–2086.

Lewin B. 1980. Gene expression. New York: John Wiley and Sons. pp. 360–362.

Maga G, Hubscher U. 2003. Proliferating cell nuclear antigen (PCNA): A dancer with many partners. J Cell Sci 116:3051–3060.

Maya-Mendoza A, Aranda-Anzaldo A. 2003. Positional mapping of specific DNA sequences relative to the nuclear substructure by direct polymerase chain reaction on nuclear matrix-bound templates. Anal Biochem 313:196–207.

Maya-Mendoza A, Hernández-Muñoz R, Gariglio P, Aranda-Anzaldo A. 2003. Gene positional changes relative to the nuclear substructure correlate with the proliferating status of hepatocytes during liver regeneration. Nucleic Acids Res 31:6168–6179.

Maya-Mendoza A, Hernández-Muñoz R, Gariglio P, Aranda-Anzaldo A. 2004. Gene positional changes relative to the nuclear substructure during carbon tetrachloride-induced hepatic fibrosis in rats. J Cell Biochem 93: 1084–1098.

Maya-Mendoza A, Hernández-Muñoz R, Gariglio P, Aranda-Anzaldo A. 2005. Natural ageing in the rat liver correlates with progressive stabilisation of DNA-nuclear matrix interactions and withdrawal of genes from the nuclear substructure. Mech Ageing Dev 126:767–782.

Michalopoulos GK, DeFrances MC. 1997. Liver regeneration. Science 276: 60–66.

Mika S, Rost B. 2005. NMPdb: Database of nuclear matrix proteins. Nucleic Acids Res 33:D160–D163.

Morales-González JA, Gutiérrez-Salinas J, Yánez L, Villagómez-Rico C, Badillo-Romero J, Hernández-Muñoz R. 1999. Morphological and biochemical effects of a low ethanol dose on rat liver regeneration. Dig Dis Sci 44:1963–1974.

Nakamura H, Morita T, Sato C. 1986. Structural organizations of replicon domains during DNA synthetic phase in the mammalian nucleus. Exp Cell Res 165:291–297.

Nickerson JA. 2001. Experimental observations of a nuclear matrix. J Cell Sci 114:463–474.

Ottaviani D, Lever E, Takousis P, Sheer D. 2008. Anchoring the genome. Genome Biol 9(1):201.

Radulescu AE, Cleveland DW. 2010. NuMA after 30 years: The matrix revisited. Trends Cell Biol 20:214–222.

Razin SV. 1997. Nuclear matrix and the spatial organization of chromosomal DNA domains. Austin: RG Landes Co. Inc. p. 13.

Razin SV. 2001. The nuclear matrix and chromosomal DNA loops: Is there any correlation between partitioning of the genome into loops and functional domains? Cell Mol Biol Lett 6:59–69.

Rivera-Mulia JC, Aranda-Anzaldo A. 2010. Determination of the *in vivo* structural DNA loop organization in the genomic region of the rat albumin locus by means of a topological approach. DNA Res 17: 23–35.

Rivera-Mulia JC, Hernández-Muñoz R, Martínez F, Aranda-Anzaldo A. 2011. DNA moves sequentially towards the nuclear matrix during DNA replication in vivo. BMC Cell Biol 12:3.

Roti-Roti JL, Wright WD, Taylor YC. 1993. DNA loop structure and radiation response. Adv Radiat Biol 17:227–259.

Sadoni N, Cardoso MC, Stelzer EH, Leonhardt H, Zink D. 2004. Stable chromosomal units determine the spatial and temporal organization of DNA replication, J Cell Sci 117:5353–5365.

Simon DN, Wilson KL. 2011. The nucleoskeleton as a genome-associated dynamic network of networks. Nat Rev Mol Cell Biol 12:695–708.

Taub R. 1996. Transcriptional control of liver regeneration. FASEB J 10:413–427.

Tomilin N, Solovjeva L, Krutilina R, Chamberland C, Hancock R, Vig B. 1995. Visualization of elementary DNA replication units in human nuclei corresponding in size to DNA loop domains. Chromosome Res 3:32–40.

Trevilla-García C, Aranda-Anzaldo A. 2012. The organization of a large transcriptional unit (*Fyn*) into structural DNA loops is cell-type specific and independent of transcription. Gene 493:1–8.

Tsutsui KM, Sano K, Tsutsui K. 2005. Dynamic view of the nuclear matrix. Acta Med Okayama 59:113–120.

Verheijen R, Kuijpers H, Vooijs P, van Venrooij W, Ramaekers F. 1986. Protein composition of nuclear matrix preparations from HeLa cells: An immunochemical approach. J Cell Sci 80:103–122.

Wei X, Samarabandu J, Devdhar RS, Siegel AJ, Acharya R, Berezney R. 1998. Segregation of transcription and replication sites into higher order domains. Science 281:1502–1506.

Woodcock CL, Ghosh RP. 2010. Chromatin higher-order structure and dynamics. Cold Spring Harbor Perspect Biol 2:a000596.